Structural change of the tunneling spectrum with perturbation frequency

2010 J. Phys. A: Math. Theor. 43 192001

(http://iopscience.iop.org/1751-8121/43/19/192001)

IOP FTC
IOP PUBLISHING JOURNAL OF PHYSICS A: MATHEMATICAL AND THEORETICAL

J. Phys. A: Math. Theor. **43** (2010) 192001 (10pp) doi:10.1088/1751-8113/43/19/192001

FAST TRACK COMMUNICATION

Structural change of the tunneling spectrum with perturbation frequency

K Takahashi[1] **and K S Ikeda**[2]

[1] The Physics Laboratories, Kyushu Institute of Technology, Kawazu 680-4, Iizuka 820-8502, Japan
[2] Department of Physics, Ritsumeikan University, Noji-higashi 1-1-1, Kusatsu 525-8577, Japan

E-mail: takahasi@mse.kyutech.ac.jp

Received 13 January 2010, in final form 8 March 2010
Published 23 April 2010
Online at stacks.iop.org/JPhysA/43/192001

Abstract
We investigate in what regime of the frequency the new tunneling mechanism using unstable and stable manifolds of dividing saddle (Takahashi and Ikeda 2008 *J. Phys. A: Math. Theor.* **41** 095101; Takahashi and Ikeda 2009 *Phys. Rev.* A **79** 052114) works as the leading mechanism of multi-dimensional barrier tunneling. In the large and small limits of the frequency, the tunneling rate is well evaluated based on the instanton picture. It is in the intermediate frequency range that the new mechanism dominates the tunneling process. The tunneling rate takes the maximum value in this intermediate range.

PACS numbers: 05.45.Mt, 03.65.Xp, 03.65.Sq, 05.45.−a

(Some figures in this article are in colour only in the electronic version)

1. Introduction

Recent progress in the semiclassical description of tunneling in multi-dimensional systems [1–3] forces some essential alteration to understanding the basic mechanism of tunneling. For multi-dimensional barrier systems, we discovered a new semiclassical mechanism for tunneling [4–6], which is essentially different from the well-known instanton mechanism [7]. The presence of the same mechanism was later reconfirmed in [8] in a slightly different situation. In this new mechanism, trajectories contributing to tunneling are guided by complexified stable and unstable manifolds of the saddle orbit above the top of a potential barrier, for brevity called SUMGT (stable–unstable manifold guided tunneling). It was also confirmed that, if chaos exists in the real space, complexified stable and unstable manifolds of chaos guide tunneling trajectories [9, 10], and it may provide a unified theoretical

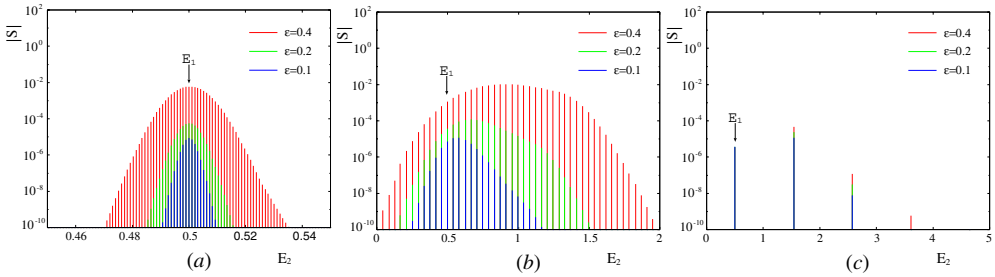

Figure 1. Change of tunneling spectra (absolute value of the S-matrix) with ω at $\epsilon = 0.1$, $\epsilon = 0.2$, $\epsilon = 0.4$ and at $\hbar = 1000/(3\pi \times 2^{10}) \sim 0.1036$. The input energy is chosen as $E_1 = 0.5$ and E_2 is the output energy. (a) $\omega = 0.01$. (b) $\omega = 0.4$. (c) $\omega = 10.0$.

understanding for various novel tunneling phenomena peculiar to multi-dimensional systems, including chaos-assisted and resonance-assisted tunneling [1–3, 11–16].

In the previous paper [6], taking a periodically perturbed 1D barrier system as a model, we reported the observability of crossover between the two different types of tunneling mechanisms, namely instanton and SUMGT, as a characteristic change in the shape of the tunneling spectrum with change of the perturbation strength. Further, we have introduced simple tools to judge which mechanism, SUMGT or instanton, dominates the tunneling process for given parameters and initial condition and to estimate the tunneling rate without going into the full detailed semiclassical calculation and analysis implemented in [5].

In this communication, we will show the outline of derivation of those simple tools, since we showed only the results without derivation in [6], and we will, by using them, investigate the change of the underlying tunneling mechanism in the whole range of perturbation frequency from a nearly zero to an extremely large value, which is an important problem but has not yet been completely analyzed [17]. There we observe significant transitions with frequency, among which SUMGT dominates in a middle range, though the time-averaged instanton and single instanton work in low and high frequency limits, respectively.

2. Model and quantum calculation

The model system adopted in this communication is the periodically perturbed Eckart barrier, which we have been using in the previous works [5, 6]:

$$\hat{H}(Q, \hat{P}, \omega t) = \tfrac{1}{2}\hat{P}^2 + (1 + \epsilon \sin \omega t)\,\mathrm{sech}^2(Q). \tag{1}$$

We assume that a plane wave with a constant input energy at $E_1 = 0.5$ is incident on this potential.

First, we show in figure 1 the results of quantum calculations at several representative perturbation frequencies. For the quantum calculations, we have used the scheme developed based on Miller's (quantum) S-matrix formula [18] by ourselves in [19], which generates an incident plane wave at a high degree of accuracy with exponentially small errors so that a scattering eigenstate is obtained numerically. The resultant tunneling spectrum as a function of the output energy E_2 (the absolute value of the S-matrix shown in figure 1) consists of delta spikes with an interval $\hbar\omega$ due to the periodicity of the perturbation, and so the interval changes with ω, where the spectrum is normalized such that $\sum_n |S(E_2 = E_1 + n\hbar\omega)|^2$ is the total transmissive probability.

For a low frequency at $\omega = 0.01$, the spectrum is localized in a very narrow range around E_1 at all three values of ϵ, i.e. $\epsilon = 0.1, 0.2, 0.4$. The shape of the spectrum and tunneling amplitude are predicted by an approximation based on instanton.

For a middle frequency at $\omega = 0.4$, the spectra at $\epsilon = 0.4$ and $\epsilon = 0.2$ form plateau envelopes spreading over wide ranges of energy, whose width is roughly estimated as $1 - \epsilon < E_2 < 1 + \epsilon$ and corresponds to the oscillating range of real unstable manifold at an asymptotic side ($|Q| \gg 1$). As reported in the previous works [5, 6], those spectra are the results of SUMGT. On the other hand, the spectrum at $\epsilon = 0.1$ is a superposition of two characteristic spectra, a head lobe explained by perturbed instanton theory and a shoulder formed over an upper range of energy as a result of SUMGT [6]. The side shoulder grows with increase of ω, then it changes into a plateau spectrum at a higher frequency ω. The growth of the shoulder also depends on ϵ: the larger the ϵ, the faster the shoulder grows with ω; then the spectrum of the strong perturbation first changes from a localized one to a plateau through intermediate spectra with a side shoulder and the spectra for the middle and weak perturbations follow successively.

For a high frequency at $\omega = 10.0$, the peak interval $\hbar\omega$ is larger than the energy difference between the potential height at rest and the input energy, i.e. $1 - E_1$; then the semiclassical approximation may not be available in this case. Each peak of the spectrum is separated from others, and the heights of peaks at the same energy value are not much different for the three values of ϵ. The peaks at excited energy levels, i.e. $E_2 = E_1 + n\hbar\omega$ ($n \geqslant 1$), rapidly decay with ω; then at $\omega \geqslant 30.0$, only the peak at the input energy E_1 appears in our numerical range. This means that the spectrum converges to that of the unperturbed system irrespective of ϵ.

Consequently, the quantum calculations show that the shape and energy range of spectrum change drastically with the increase of ω and so the whole frequency range is separated into three characteristic ranges, in which the spectrum behaves differently. It indicates that there are at least three characteristic mechanisms successively governing the tunneling process with the change of ω.

3. Semiclassical analysis

The semiclassical S-matrix [18, 20] is given by

$$S(E_2, E_1) \sim \lim_{Q_1, |Q_2| \to \infty} \sum_{\text{c.t.}} \frac{\sqrt{|P_2||P_1|}}{\sqrt{2\pi i\hbar P_1 P_2}} \sqrt{-\frac{\partial^2 S_S}{\partial E_1 \partial E_2}}\, \mathrm{e}^{-\frac{i}{\hbar}(P_2 Q_2 - P_1 Q_1)}\, \mathrm{e}^{\frac{i}{\hbar} S_S(Q_2, E_2, Q_1, E_1)}, \tag{2}$$

where the classical action is defined by

$$S_S = \int_{Q_1}^{Q_2} P\, \mathrm{d}Q - \int_{t_1}^{t_2} H(Q, P, \omega t)\, \mathrm{d}t + E_2 t_2 - E_1 t_1. \tag{3}$$

The summation $\sum_{\text{c.t.}}$ is taken over all the contributing trajectories satisfying the input and output boundary conditions [18, 20]. The coordinate Q_i and the momentum P_i (or energy $E_i = P_i^2/2$) at the input side ($i = 1$) and at the output side ($i = 2$) are the quantities observed and should be taken as real values, whereas times t_i are unobserved and are allowed to be *complex* variables. Then, the initial and final manifolds are respectively defined by

$$\mathcal{I} = \{(t_1, Q, P) | t_1 \in \mathbf{C}, Q = Q_1, P = P_1 (= -\sqrt{2E_1})\} \tag{4}$$

and

$$\mathcal{F} = \{(t_2, Q, P) | t_2 \in \mathbf{C}, Q = Q_2, P = P_2 (= -\sqrt{2E_2})\}, \tag{5}$$

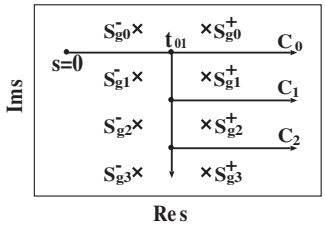

Figure 2. Singularities and representative integration paths on the lapse time plane.

which determine isolated (real and/or complex) trajectories. In practical calculation, we can regard (Q, P) as functions of the lapse time $s \equiv t - t_1 (\in \mathbf{C})$, the initial time $t_1 (\in \mathbf{C})$ and the set of fixed initial values $(Q_1, P_1) (\in \mathbf{R^2}, Q_1 > 0)$, so that t_1 is taken as a complex search parameter to find trajectories satisfying the output boundary condition, i.e. $Q = Q_2$ (fixed) and $E_2 \in \mathbf{R}^+$ (positive real) [20].

The classical solution of the unperturbed system at $\epsilon = 0$ is given for $0 < E_1 < 1$ by

$$Q(t) = \sinh^{-1}(\lambda \cosh(\sqrt{2E_1}(t - t_0))), \tag{6}$$

where $\lambda \equiv \sqrt{1/E_1 - 1}$ and t_0 is the time at which the trajectory hits the turning point [18, 20]. Given the initial condition $(Q = Q_1 (\gg 1), P = P_1 (= -\sqrt{2E_1} < 0))$ at $t = t_1$, the interval between t_0 and t_1 is given by $t_0 - t_1 = (Q_1 - \log \lambda)/\sqrt{2E_1} \equiv t_{01}$.

As shown in figure 2, the solution has singularities in the lapse time plane and the singularities are aligned along two vertical lines, i.e. the entrance singularities Sg_n^-'s and the exit singularities Sg_n^+'s. The distances between the singularities are given as follows: $\left|Sg_n^{\pm} - Sg_{n+1}^{\pm}\right| = \pi/\sqrt{2E_1}$ and $Sg_n^+ - Sg_n^- = 2\frac{1}{\sqrt{2E_1}}\sinh^{-1}(1/\lambda)$. Figure 2 also shows representative integration paths labeled 'C_n'(n: integer), which are different in topology. Trajectories defined along integration paths homotopic to C_{2n+1}'s make contributions to the tunneling component, while trajectories along C_{2n}'s go back to the reflective side [4, 20]. The path C_1 makes a dominant contribution for the tunneling rate because it has the shortest imaginary time evolution giving the smallest imaginary part in classical action among all odd number integration paths C_{2n+1}'s. The complex trajectory with imaginary time evolution along the vertical part of C_1 is called 'instanton' [7] and the imaginary depth of instanton is determined by $t_{\mathrm{inst}}(E_1) = -\pi/\sqrt{2E_1}$ [6]. Then, the tunneling amplitude is estimated by

$$W_I = \exp\left(-\frac{1}{\hbar}\,\mathrm{Im}\, S_{I0}\right), \tag{7}$$

where the imaginary part of the classical action $\mathrm{Im}\, S_{I0}$ along instanton is given by

$$\mathrm{Im}\, S_{I0} = \sqrt{2E_1}\,\frac{1 - E_1}{E_1 + \sqrt{E_1}}. \tag{8}$$

Even when a non-zero perturbation is applied to the system, the topology of integration paths is roughly characterized by that of the unperturbed system at $\epsilon = 0$ in the case when the instanton picture works well [4, 5]. In the low frequency limit $\omega \to 0$, the adiabatic approximation based on instanton can be available. In this case, the effective imaginary time evolution of instanton may be given by $t_{\mathrm{inst}}(E) = -\pi/\sqrt{2E}$ at $E \sim E_1 + \epsilon$, i.e. the shortest imaginary path during the period of perturbation, but the tunneling amplitude is, as shown later, estimated more precisely by the time average of instantaneously instanton weights [6]:

$$W_{\mathrm{av}} = \frac{1}{T}\int_0^T \exp\left(-\frac{1}{\hbar}\,\mathrm{Im}\, S_I\right) \mathrm{d}t, \tag{9}$$

where

$$\mathrm{Im}\, S_I = \sqrt{2E_1}\frac{a(t) - E_1}{E_1 + \sqrt{a(t)E_1}} \tag{10}$$

with $a(t) = 1 + \epsilon \sin \omega t$, the time-dependent barrier height.

On the other hand, the different semiclassical mechanism, SUMGT, dominates the averaged instanton for the middle frequency range. In this case, trajectories contributing to tunneling go along the complexified stable manifold of the unstable periodic orbit on the top of an oscillating potential barrier in the reactant side and are scattered along the unstable manifold of it in the product side. Actually, a certain critical trajectory on the stable manifold W_s guides those tunneling trajectories and its initial point t_{1c}, the so-called critical point, is the intersection of the initial manifold $\mathcal{I}$ with the stable manifold W_s.

The existence of the critical point can be proved by using the Melnikov method [4, 21]. Actually, the energy of a trajectory on the stable manifold at a given time t can be evaluated by

$$H(Q_s(t), P_s(t), \omega t) = H(Q_{\mathrm{ups}}(t), P_{\mathrm{ups}}(t), \omega t) - \int_t^\infty \left\{ \frac{\partial V}{\partial t'}(Q_s(t'), \omega t') - \frac{\partial V}{\partial t'}(Q_{\mathrm{ups}}(t'), \omega t') \right\} \mathrm{d}t', \tag{11}$$

where $V(Q, \omega t) = (1 + \epsilon \sin \omega t)\mathrm{sech}^2 Q$, $(Q_{\mathrm{ups}}, P_{\mathrm{ups}})$ denotes the unstable periodic orbit, and (Q_s, P_s) denotes a trajectory on the stable manifold. At the first-order approximation of $O(\epsilon)$, namely the Melnikov method [21], the solution $Q_s(t)$ in equation (11) is replaced by the unperturbed solution Q_{s0} on the stable manifold [4],

$$Q_{s0}(t) = \sinh^{-1}(\mathrm{e}^{-\sqrt{2}(t-\mu)}), \tag{12}$$

where the parameter μ indicates the initial phase or initial time of the solution. Note that in the Melnikov method, we use the solution on the stable manifold, and so the time plane topology of the trajectory is much simpler than those of SUMGT trajectories due to the divergence movement of the singularities Sg_n^+'s at the critical point. Namely, as shown in [4] and [5], the singularities Sg_n^+'s diverge at the critical point, though the singularities Sg_n^-'s remain almost at the same positions. The integration path is taken such that it starts at the complex initial time t_1, passes between Sg_0^- and Sg_1^- and goes toward the real positive infinity, but any homotopic deformations are possible. So it is simply taken as $t_1 \to \mu \to t_2 + \mathrm{Im}\, t_1 \to t_2 (\in \mathbf{R})$, where $\mathrm{Im}\, \mu = \mathrm{Im}\, t_1$ and $t_2 \to +\infty$. Since $H(Q_s(t), P_s(t), \omega t)$ converges to $H(Q_{\mathrm{ups}}(t), P_{\mathrm{ups}}(t), \omega t)$ in the limit $\mathrm{Re}\, t \to +\infty$, then equation (11) is integrated analytically and the energy at the initial time t_1 is given as a function of μ [4]:

$$H(t_1) \sim 1 + \epsilon(1 - \chi(\omega)) \sin \omega\mu + O(\epsilon^2), \tag{13}$$

where $\chi(\omega)$ is defined by

$$\chi(\omega) \equiv 2\omega \int_0^\infty \frac{\sin \omega s}{1 + \mathrm{e}^{2\sqrt{2}s}}\, \mathrm{d}s, \tag{14}$$

and μ is related to t_1 as $\mu \equiv t_1 + (Q_1 - \log 2)/\sqrt{2}$. On the initial plane $\mathcal{I}$, the initial energy E_1 should take a real value. If E_1 $(\in \mathbf{R}^+)$ is taken such that $E_1 < 1 - \epsilon(1 - \chi(\omega))$, i.e. the tunneling case, the intersection t_{1c} between W_s and $\mathcal{I}$ occurs in the complex domain and its imaginary part is given by

$$\mathrm{Im}\, t_{1c} = \frac{1}{\omega} \cosh^{-1} \left\{ \frac{1 - E_1}{\epsilon(1 - \chi(\omega))} \right\}. \tag{15}$$

Then, $\mathrm{Im}\, t_{1c}$ decreases with the increase of ω and/or ϵ.

The semiclassical weights of SUMGT trajectories are evaluated by

$$W_S = \hbar\omega \exp\left(-\frac{1}{\hbar}\,\mathrm{Im}\,S_S\right), \tag{16}$$

where the coefficient $\hbar\omega$ arises from the spike density of the spectrum with the interval $\hbar\omega$ [20]. The values of $\mathrm{Im}\,S_S$ for SUMGT trajectories are well approximated by that of the critical trajectory starting at t_{1c} because the major contributing trajectories of SUMGT start from a very small neighborhood of t_{1c} and are guided by the critical trajectory until being close to the unstable periodic orbit. As remarked above, the time plane topology of the critical trajectory is much simpler than those of SUMGT trajectories due to the divergence behavior of the singularities Sg_n^+'s [4, 5]; then the evaluation of $\mathrm{Im}\,S_S$ becomes easier. Actually, $\mathrm{Im}\,S_S$ of the critical trajectory can be evaluated using the Melnikov method [6]. To do this, the classical action is rewritten as follows:

$$S_S(Q_2, E_2, Q_1, E_1) = \int_{t_1}^{t_2} H(Q, P, \omega t)\,\mathrm{d}t - \int_{t_1}^{t_2} 2V(Q, \omega t) + E_2 t_2 - E_1 t_1. \tag{17}$$

The time evolution of the Hamiltonian $H(Q, P, \omega t)$ is given by equation (11). According to the usual way of the Melnikov method [21], the classical variables $Q(t)$ and $P(t)$ are replaced by those of the unperturbed trajectory on the stable manifold. Taking the integration path as $t_{1c} \to t_2' \to t_2 (\in \mathbf{R})$, where $\mathrm{Im}\,t_{1c} = \mathrm{Im}\,t_2'$ and $\mathrm{Re}\,t_2' = t_2 \to +\infty$, we, after some calculations, obtain the expression of $\mathrm{Im}\,S_S$ [6],

$$\begin{aligned}\mathrm{Im}\,S_S \sim{}& \mathrm{Im}\,t_{1c}(1 - E_1) - \frac{1 - E_1}{\omega}\frac{\sinh(\omega\,\mathrm{Im}\,t_{1c})}{\cosh(\omega\,\mathrm{Im}\,t_{1c})} \\ &+ \sqrt{2}\sinh(\omega\,\mathrm{Im}\,t_{1c})\int_{\infty}^{0}\mathrm{d}x\int_{\infty}^{x}\mathrm{d}s\,\frac{\epsilon\sin\omega s}{\cosh^2(\sqrt{2}s)} + O(\epsilon^2),\end{aligned} \tag{18}$$

which allows us to calculate the tunneling weight through equation (16).

The threshold value ω_{ci} at which the transition between instanton and SUMGT occurs is simply determined by comparison of the imaginary depth of instanton $|t_{\mathrm{inst}}(E = E_1 + \epsilon)|$ with the imaginary part of the critical point $\mathrm{Im}\,t_{1c}$. Figure 3 shows $\mathrm{Im}\,t_{1c}$ as a function of ω at $\epsilon = 0.1, 0.2, 0.4$ together with $|t_{\mathrm{inst}}(E_1 + \epsilon)|$. $t_{\mathrm{inst}}(E_1 + \epsilon)$ is independent of ω and does not so much change with ϵ. On the other hand, $\mathrm{Im}\,t_{1c}$ decreases as $\propto 1/\omega$ for the range $\omega < 1$, and it becomes smaller with the increase of ϵ at each fixed ω in this range. In the limit $\omega \to \infty$, $\mathrm{Im}\,t_{1c}$, however, converges irrespective of ϵ to a constant, $\mathrm{Im}\,t_{1c} \to \frac{\pi}{2\sqrt{2}}$, which is always less than $|t_{\mathrm{inst}}(E_1 + \epsilon)|$. Then the intersection of $\mathrm{Im}\,t_{1c}$ with $|t_{\mathrm{inst}}(E_1 + \epsilon)|$ always exists for any perturbation strength if $\epsilon < 1 - E_1$, but the intersections for $\epsilon = 0.1$, 0.2 and 0.4, say ω_{ci1}, ω_{ci2} and ω_{ci4}, hold the relation $\omega_{\mathrm{ci4}} < \omega_{\mathrm{ci2}} < \omega_{\mathrm{ci1}}$. In the range $\omega < \omega_{ci}$, instanton should dominate the tunneling process, but out of this range SUMGT may take the place of instanton.

In figure 4, the maximum value of the peaks of the quantum tunneling spectrum, $\max|S|$, namely the tunneling amplitude, at $\epsilon = 0.1, 0.2, 0.4$ is plotted as a function of ω, where the incident plane wave is normalized such that $|S|^2 = 1$ for the free particle without any potential. In figure 4, the semiclassical weight of instanton without perturbation, W_I, that of averaged instanton W_{av} and that of SUMGT W_S are also drawn for comparison.

In the range $\omega < \omega_{ci}$, the weight of averaged instanton W_{av} reproduces the quantum results, which converge to different constant values at $\epsilon = 0.1, 0.2, 0.4$ in the limit $\omega \to 0$. On the other hand, in the range $\omega_{ci} < \omega < \omega_{cq}$, the SUMGT weight W_S takes the maximum at a certain value of ω and follows the quantum results ignoring small oscillations, where $\omega_{\mathrm{cq}} \equiv \frac{1-E_1}{\hbar}$ is the frequency above which the particle gains a piece of energy to go beyond the potential barrier by absorbing a single quanta $\hbar\omega$. It is in this range that the tunneling

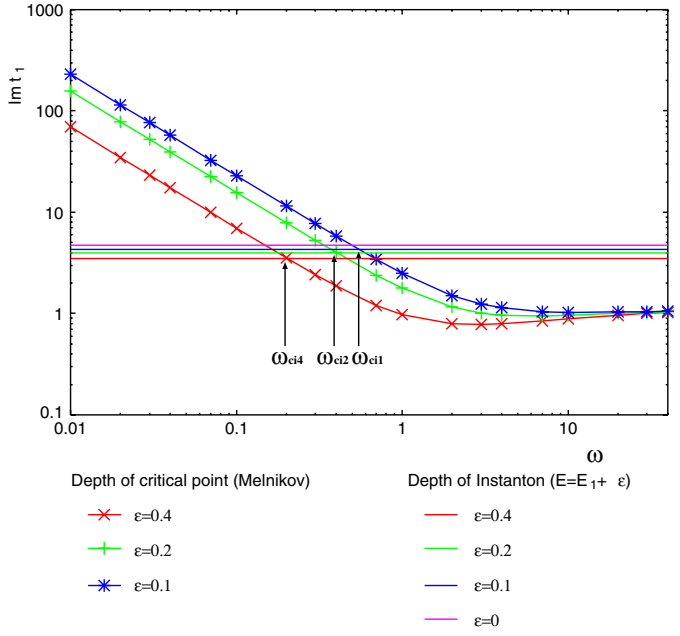

Figure 3. Depth of the critical point versus the depth of instanton with ω.

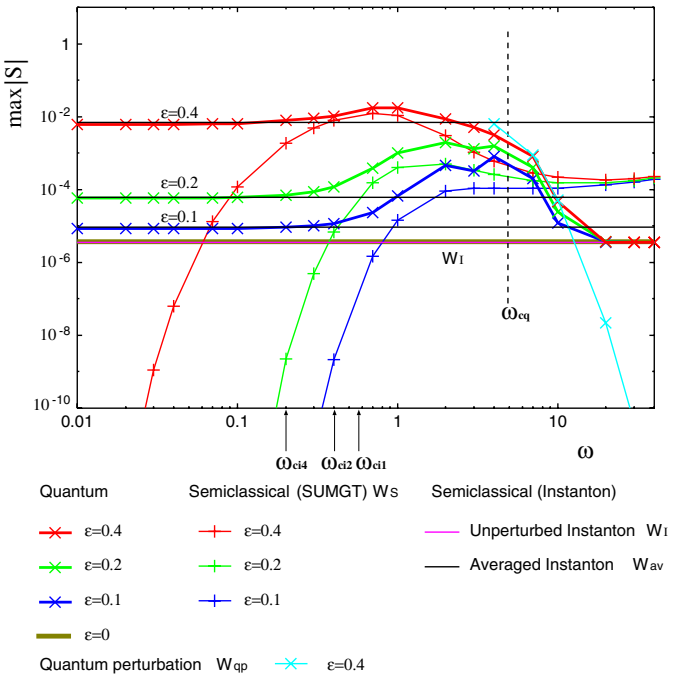

Figure 4. Comparison of semiclassical predictions by SUMGT and instanton with quantum calculation in the maximum height of the spectrum.

spectrum forms a plateau manifesting the direct influence of the unstable manifold as shown in figure 1(*b*) [5, 6]. It is quite interesting that the maximum value of tunneling amplitude in the range $\omega_{\rm ci} < \omega < \omega_{cq}$ becomes more than ten times (or hundred times) larger than $W_{\rm av}$ for $\epsilon = 0.2$ and 0.1, though it is slightly larger than $W_{\rm av}$ at $\epsilon = 0.4$. It means that the effect of SUMGT is magnified for weak perturbations rather than for strong ones. We are now studying this problem for future publication. Note that the discrepancy between the quantum calculation and the SUMGT weight W_S seems to increase with decrease of ϵ. It mainly comes from ignoring the amplitude factor in equation (2), i.e. $\sqrt{-\frac{\partial^2 S_S}{\partial E_1 \partial E_2}}$. Indeed, as shown in [5], the order of the amplitude factor is estimated as $\sqrt{1/(\epsilon\omega)}$ in a low frequency range ($\omega < 1$) and takes larger values for smaller ϵ's. We do not have any simple evaluation in a high frequency range ($\omega > 1$), but we believe that it is also attributed to neglect of the amplitude factor.

In the range $\omega > \omega_{\rm cq}$, SUMGT is no longer available except for a border region near $\omega_{\rm cq}$. Indeed, the maximum of quantum spectrum rapidly decreases with ω and converges to that of the unperturbed system well estimated by W_I. It means that the frequency is too high for the particle to gain any energy in the limit $\omega \to \infty$. On the other hand, the imaginary part of S_S of the critical trajectory seems to converge to a constant value,

$$\lim_{\omega\to\infty} \mathrm{Im}\, S_S = (1 - E_1)\pi/\sqrt{2}, \tag{19}$$

so that W_S turns to increase with ω as $\propto \omega$ (see equation (16)) after a rapid decrease in a short interval of ω above $\omega_{\rm cq}$ and is always larger than W_I for $\omega > \omega_{\rm cq}$. In the range $\omega \gg \omega_{cq}$, the energy of the state excited by absorbing a single quanta $\hbar\omega$, i.e. $E = E_1 + \hbar\omega$, exceeds the characteristic energy range of the unstable manifold $1 - \epsilon < E < 1 + \epsilon$ ($\epsilon < 1 - E_1$), which means that there is no spectrum peak in this energy range. Therefore, the SUMGT approximation does not work. In this regime, the quantum perturbation method should be available. In practice, the escaping amplitude due to the absorption of the quanta $\hbar\omega$ can be roughly estimated by

$$\begin{aligned} |S(E_1 + \hbar\omega)| &\sim \epsilon\pi C_\omega | < u_{E_1+\hbar\omega} | V_0(Q) | u_{E_1} > | \\ &\equiv W_{\rm qp}, \end{aligned} \tag{20}$$

where u_E is the scattering eigenstate of the unperturbed system, $V_0(Q) = \mathrm{sech}^2(Q)$ and

$$C_\omega = \left\{ \sinh^2\left(\frac{\pi}{\hbar}\sqrt{2E'}\right) \Big/ \left[\sinh^2\left(\frac{\pi}{\hbar}\sqrt{2E'}\right) + \cosh^2\left(\frac{\pi}{2}\sqrt{\frac{8}{\hbar^2} - 1}\right) \right] \right\}^{1/2} \tag{21}$$

with $E' = E_1 + \hbar\omega$. This component is nothing more than the so-called photo-assisted tunneling amplitude, which shows a good agreement with the quantum calculation as shown in figure 4, but it decreases exponentially with ω and is finally replaced by the instanton tunneling amplitude W_I (also see figure 4).

4. 2D system

Finally, we mention that the characteristic changes of tunneling spectra described above occur in a 2D autonomous barrier system such as [5]

$$\hat{H}_{\rm tot}(Q, \hat{P}, q, \hat{p}) = \tfrac{1}{2}\hat{P}^2 + (1 + \beta q)\mathrm{sech}^2 Q + \hat{H}_{\rm ch}(q, \hat{p}), \tag{22}$$

where $\hat{H}_{\rm ch}$ denotes the Hamiltonian of a harmonic channel given by $\hat{H}_{\rm ch}(q, \hat{p}) = \frac{1}{2}\hat{p}^2 + \frac{1}{2}\omega^2 q^2$. It provides a simplified model of collinear atom–diatomic molecule collisions [13, 18], where the harmonic channel imitates the diatomic molecular vibration. In the limit $\beta = 0$, the system is separable: the reaction degree of freedom (Q, P) and channel degree of freedom (q, p). The quantum and classical dynamics of the reaction degree of freedom are completely described

by those of the unperturbed system of equation (1) with $\epsilon = 0$. Even when the channel energy is highly excited such that the total energy $E_{\rm tot} = H_{\rm tot}$ is larger than the potential energy at its saddle point $(Q, q) = (0, -\beta/\omega^2)$, instanton-type tunneling is observed for a sufficiently small initial energy of the reaction degree of freedom. One can easily confirm that the 2D system (22) has a periodic saddle at $(Q, P) = (0, 0)$, i.e. a harmonic vibration of the channel, which is just the 1D normally hyperbolic invariant manifold [22]. The saddle has the same stable and unstable manifolds in the reaction degree of freedom like the 1.5D model (1) (see equation (12)).

For a non-zero but not so strong perturbation ($\beta \neq 0$), the channel vibration plays the role of a periodic force of the 1.5D system if the initial channel energy (eigenvalue of $\hat{H}_{\rm ch}$) is sufficiently large. Indeed, the energy exchange between the reaction and channel degrees of freedom in the collision process is negligibly small compared with the initial channel energy; then the motion of the channel is well approximated by the unperturbed channel vibration, i.e. harmonic oscillator. In this case, the parameter β plays the role of ϵ and the channel frequency ω corresponds to the perturbation frequency of the 1.5D system in equation (1). Thus, the theoretical results so far developed for the non-autonomous model (1) are valid for the 2D autonomous model (22) [5]. The complex domain Melnikov-like perturbation theory developed for the non-autonomous model can be straightforwardly extended to the 2D model without any modification. We can predict the intersection of the stable manifold with the initial manifold (initial channel eigenstate) in the complex domain, and estimate the tunneling amplitude for the 2D system in the same way. So tunneling caused by SUMGT, i.e. plateau spectrum, arises in certain parameter ranges. As a result, the observed tunneling spectrum of the 2D model exhibits changes with change of ω similar to figure 1. The details will be reported in forthcoming papers.

Note that in the regime of the true energy-barrier tunneling, namely $E_{\rm tot}$ less than the saddle of the potential, the unstable periodic orbit will be bifurcated into a complex one. It is expected from quantum calculations in [13] and from our preliminary quantum calculation that SUMGT makes less contribution and instanton-type tunneling dominates, even if an entanglement of the stable manifold with the initial manifold exists. So we do not discuss this case.

5. Conclusion

In conclusion, we claim that there are three ranges of perturbation frequency in which the tunneling effect is qualitatively different to each other. In the low frequency range ($\omega < \omega_{\rm ci}$), the adiabatic approximation based on instanton, i.e. averaged instanton, works well, which is expected from some other works [17]. In the middle frequency range ($\omega_{\rm ci} < \omega < \omega_{\rm cq}$), which is the inherently multi-dimensional regime, SUMGT governs the tunneling process instead of instanton. In a high range ($\omega > \omega_{\rm cq}$), tunneling converges to that of the unperturbed system, i.e. the unperturbed instanton, but the transition from SUMGT to the unperturbed instanton observed in a short frequency range is well approximated by the quantum perturbation method.

The formation of the plateau spectrum by the SUMGT mechanism and spectrum transformation caused by the switching of mechanism from the SUMGT to instanton are quite universal phenomena, and they will certainly be observed in numerical simulation of more realistic models, which will be reported in forthcoming papers. Moreover, we expect that plateau-type spectrum and spectrum transformation will be observed in actual experiments such as molecule–molecule or molecule–atom collision processes. In particular, plateau-like spectra have been observed in the experiments of the above-threshold ionization of Rydberg atoms and the connection with our theory is quite interesting [23].

Acknowledgments

The present work is supported by Grant-in-Aid for Scientific Research (B) No 20340100 from JSPA.

References

[1] Tomsovic S (ed) 1998 *Tunneling in Complex Systems* (Singapore: World Scientific)
[2] Ankerhold J 2007 *Quantum Tunneling in Complex Systems: The Semiclassical Approach* (Berlin: Springer)
[3] Keshavamurthy S 2007 *Int. Rev. Phys. Chem.* **26** 521
[4] Takahashi K, Yoshimoto A and Ikeda K S 2002 *Phys. Lett.* A **297** 370
Takahashi K and Ikeda K S 2003 *J. Phys. A: Math. Gen.* **36** 7953
[5] Takahashi K and Ikeda K S 2005 *Europhys. Lett.* **71** 193
Takahashi K and Ikeda K S 2006 *Europhys. Lett.* **75** 355
Takahashi K and Ikeda K S 2008 *J. Phys. A.: Math Theor.* **41** 095101
[6] Takahashi K and Ikeda K S 2009 *Phys. Rev.* A **79** 052114
[7] Schulman L S 1981 *Techniques and Applications of Path Integration* (New York: Wiley)
[8] Bezrukov F and Levkov D 2004 *J. Exp. Theor. Phys.* **98** 820
Levkov D G, Panin A G and Sibiryakov S M 2007 *Phys. Rev. Lett.* **99** 170407
Levkov D G, Panin A G and Sibiryakov S M 2007 *Phys. Rev.* E **76** 046209
Levkov D G, Panin A G and Sibiryakov S M 2009 *J. Phys. A: Math. Theor.* **42** 205102
[9] Shudo A and Ikeda K S 1995 *Phys. Rev. Lett.* **74** 682
Shudo A and Ikeda K S 1998 *Physica* D **115** 234
[10] Shudo A, Ishii Y and Ikeda K S 2002 *J. Phys. A: Math. Gen.* **35** L225
Shudo A, Ishii Y and Ikeda K S 2008 *Europhys. Lett.* **81** 50003
Shudo A, Ishii Y and Ikeda K S 2009 *J. Phys. A: Math. Theor.* **42** 265101
Shudo A, Ishii Y and Ikeda K S 2009 *J. Phys. A: Math. Theor.* **42** 265102
[11] Bohigas O, Tomsovic S and Ullmo D 1990 *Phys. Rev. Lett.* **65** 5
Bohigas O, Tomsovic S and Ullmo D 1993 *Phys. Rep.* **223** 45
[12] Creagh S C and Whelan N D 2000 *Phys. Rev. Lett.* **84** 4084
[13] Creagh S C 2004 *Nonlinearity* **17** 1261
Creagh S C 2005 *Nonlinearity* **18** 2089
Drew C S, Creagh S C and Tew R H 2005 *Phys. Rev.* A **72** 062501
[14] Hensinger W K *et al* 2001 *Nature* **412** 52
Steck D A, Oskay W H and Raizen M G 2001 *Science* **293** 274
Dembowski C *et al* 2000 *Phys. Rev. Lett.* **84** 867
[15] Brodier O, Schlagheck P and Ullmo D 2001 *Phys. Rev. Lett.* **87** 064101
Brodier O, Schlagheck P and Ullmo D 2002 *Ann. Phys., NY* **300** 88
Eltschka C and Schlagheck P 2005 *Phys. Rev. Lett.* **94** 014101
[16] Bäcker A, Ketzmerick R, Lock S and Schilling L 2008 *Phys. Rev. Lett.* **100** 104101
Bäcker A *et al* 2008 *Phys. Rev. Lett.* **100** 174103
Bäcker A, Ketzmerick R, Lock S, Wiersig J and Hentschel M 2009 *Phys. Rev.* A **79** 063804
[17] Büttiker M and Landauer R 1982 *Phys. Rev. Lett.* **49** 1739
Büttiker M and Landauer R 1985 *Phys. Scr.* **32** 429
[18] Miller W H 1970 *J. Chem. Phys.* **53** 1949
Miller W H and George T F 1972 *J. Chem. Phys.* **56** 5668
George T F and Miller W H 1972 *J. Chem. Phys.* **57** 2458
Miller W H 1974 *Adv. Chem. Phys.* **25** 69
[19] Takahashi K and Ikeda K S 1997 *J. Chem. Phys.* **106** 4463
[20] Takahashi K and Ikeda K S 2000 *Ann. Phys., NY* **283** 94
[21] Wiggins S 1990 *Introduction to Applied Nonlinear Dynamical Systems and Chaos* (New York: Springer)
[22] Wiggins S, Wiesenfeld L, Jaffe C and Uzer T 2001 *Phys. Rev. Lett.* **86** 5478
[23] Paulus G G, Grasbon F, Walther H, Kopold R and Becker W 2001 *Phys. Rev.* A **64** 021401